RILEM Technical Letters (2018) 3: 66-74
DOI: http://dx.doi.org/10.21809/rilemtechlett.2018.66

Utilization of volcanic ejecta as a high-performance supplementary cementitious material by gravity classification and pulverization

Atsushi Tomoyose [a*], Takafumi Noguchi [a], Kenichi Sodeyama [b], Kazuro Higashi [c]

[a] The University of Tokyo, Graduate School of Engineering, 7-3-1, Hongo, Bunkyo-ku, Tokyo 113-8656, Japan
[b] Kagoshima Prefectural Institute of Industrial Technology, 1445-1, Oda, Hayato-cho, Kirishima-shi, Kagoshima 899-5105, Japan
[c] Principle CO., LTD. 1-17-8, Kamoike, Kagoshima-shi, Kagoshima 890-0063, Japan

Received: 18 August 2018 / Accepted: 30 December 2018 / Published online: 31 December 2018

Abstract

The reaction of natural pozzolans is caused by volcanic glass composed of amorphous silicate; however, volcanic ejecta also contains crystal mineral, pumice, and sometimes weathered clay fraction in their natural conditions. By focusing on the differences of physical properties between these components, high-purity volcanic glass powder (VGP) was manufactured by dry gravity classification and pulverization. This paper reports the results of investigations to utilize pyroclastic flow deposits as a supplementary cementitious material (SCM).
Through this method, the glass content of VGP increased to 88% with a mean particle size of 1 μm, when that of the raw material is about 60%. Chemical analysis indicated that VGP is principally composed of silica (about 72%) and alumina (about 13%).
The performance of VGP as a SCM was evaluated by conducting tests on concrete mixtures, replacing 0% to 30% by weight of Portland cement by VGP with 0.2 to 0.6 water to binder ratio. VGP concrete showed better results of 7-and 28-day compressive strength compared to control concrete in all experiments. In particular, VGP demonstrated better fluidity and strength development in concrete with a low water-binder ratio in comparison to silica fume.

Keywords: Volcanic glass; Natural pozzolan; Supplementary cementitious material; High performance concrete

1 Introduction

Ancient concrete used in the Pantheon in Rome contains volcanic ejecta, which is known as pozzolana. One popular technique to reduce CO_2 emissions stemming from concrete production and construction involves the use of these natural pozzolans as SCMs [1]. Volcanic activity is common in Japan. And one of the earliest researches to use volcanic ejecta as SCM was started more than 110 years ago in Hokkaido, the northern part of Japan [2, 3]. Subsequently, many studies were done on the applications of domestic natural pozzolan as SCM, and have been recently reviewed by Cai et al. [4]. Although concrete made with volcano-related materials had been manufactured practically until 1960's, artificial materials have been chosen as a replacement. The reaction of natural pozzolans is due to volcanic siliceous glass [5], but volcanic ejecta generally comprises not only glass but also crystal mineral and clay mineral in their natural conditions [6], which may lead to typical undesirable properties of natural pozzolans; large variety, variability, and high water demand [7].

Pyroclastic flow deposits referred to as "*shirasu*" cover a wide area, forming extensive pyroclastic plateaus with a layer about 10 meters to 200 meters thick in the southern regions of Kyushu, Japan. The greatest amount of *shirasu* sediment, which is estimated to have a volume of 75 billion m^3, is the Ito pyroclastic flow (A-Ito) that erupted out of the Aira caldera 29,000 years ago. This "*Ito-shirasu*" covers an area of about 3,427 km^2, and it contains non-welded pyroclastic flow sediment, which includes crystalline mineral, amorphous silicate, and clay fraction (CF). It is said that to utilize *Ito-shirasu* as industrial resource is very difficult for these impurities.

By the classification based on the origin of the SCMs [5], *Ito-shirasu* is included in the group of unaltered pyroclastic material. There are a few practical trials to use *Ito-shirasu* as fine aggregate [8], and a house built with *Ito-shirasu* concrete won the 2017 ACI overall "Excellence" award [9]. Despite their environmental advantage, significant barriers remain to widespread adoption of *Ito-shirasu* in place of natural sand and crushed sand. Major barrier is related to the typical properties of natural pozzolans; low fluidity due to high fineness and angular particles. Replacing 70% by volume of

* Corresponding author: Atsushi Tomoyose, E-mail: tomoyose@bme.arch.t.u-tokyo.ac.jp

crushed sand with *Ito-shirasu*, both slump and slump flow values decreased in spite of increasing superplasticizer dosage and water as shown in Table 1. It was also reported that *Ito-shirasu* concrete causes higher shrinkage than control [19]. In addition, low density (2.0~2.2 g/cm^3) and high water absorption (2.5~9.2%) for fine aggregate are other barriers by laws and standards (JIS).

Table 1. Mixing proportions and fresh properties of concrete comparing *Ito-shirasu* with crushed sand as fine aggregate.

W/C	Water (kg/m^3)	s/a (%)	Fine aggregate (kg/m^3)		Superplasticizer content by weight of cement (%)	Slump flow value (cm)	Slump (cm)
			Ito-shirasu 2.11g/cm^3	Crushed sand 2.66 g/cm^3			
0.65	168	50.0	0	921	1.2	37.0	21.0
	185	43.9	447	237	1.7	29.0	16.5

In their previous research [10-13] on the total utilization of pyroclastic flow deposits as construction materials, the authors clarified that dry gravity classification is effective in dividing *Ito-shirasu* into crystalline mineral, pumice, high-purity volcanic glass, and clay fraction. Through a separating machine made by combining a gravity separator with a winnowing sorter, the amorphous content of volcanic glass increased to 88% when that of raw material is about 60%. As the mechanism of the machine is shown in Fig. 1, winnowing with the action of the vibration fluid bed can sort particles by density, particle size, and terminal velocity with low energy consumption.

This paper presents the results of investigation on the suitability of using volcanic glass powder (VGP), manufactured by dry gravity classification and pulverization, as SCMs in concrete production.

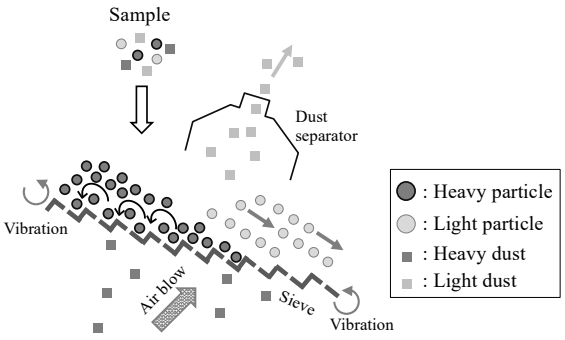

Figure 1. Mechanism of dry gravity classification.

2 Experimental program

2.1 Manufacturing process of VGP

Ito-shirasu used in this investigation was delivered from Kanoya-city, Kagoshima Prefecture in Japan by a mine operator without any pretreatment as shown in Fig. 2. The mineral composition of particle size fractions and the chemical composition of the raw material reported in the previous research [12] are presented in Fig. 3. As to mineral components, the fraction over 2.4 g/cm^3 is defined as crystalline, under 2.4 g/cm^3 defined as amorphous, and in particular under 1.5 g/cm^3 as pumice in this figure. After sieving *Ito-shirasu* to under 5 mm, *Ito-shirasu* is divided into five substances by dry gravity separator. Volcanic glass powder was manufactured through dry gravity classification and pulverization as shown in Fig. 4. First, classified volcanic glass is crushed by roller mill to a mean particle size of 5.1 µm (VGP 5). Then, VPG 5 is pulverized by a jet mill. Fine powder with a mean particle size of 1 µm (VGP 1) and coarse powder, 3 µm (VGP 3), are recovered from the bag filter and cyclone separator, respectively.

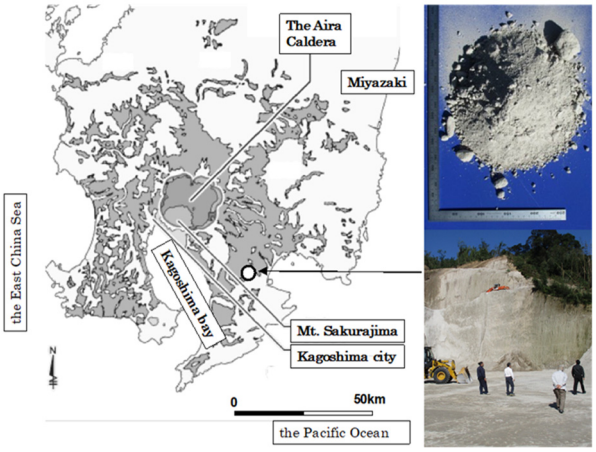

Figure 2. Distribution area of *Ito-shirasu* and sample site.

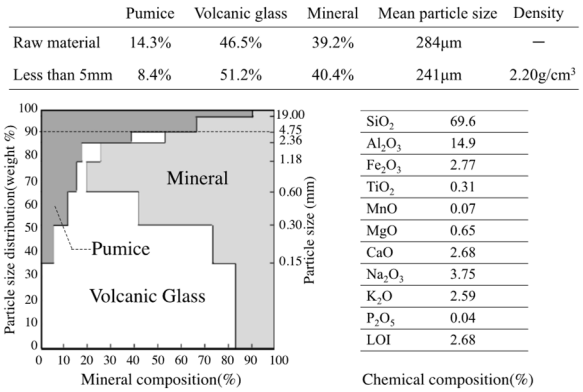

Figure 3. Properties of *Ito-shirasu* [12].

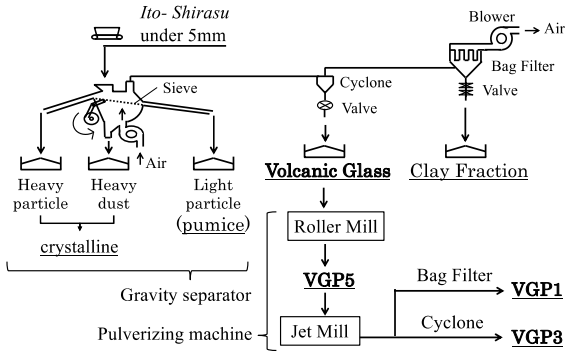

Figure 4. Manufacturing process of VGP.

2.2 Properties of VGP

The basic properties of three types of VGP are shown in Table 2; the BET specific surface area measured by N_2-adsorption, amorphous content based on heavy liquid separation using zinc bromide (ρ=2.4 g/cm^3), and chemical composition by fluorescent X-ray analysis. The SiO_2 content of VGP increased to 71.4% to 73.7% from 69.6% of that of the raw material. Besides, total alkali content of VGP is very high as well as raw material. But, previous research clarified that effective soluble amount for ASR is law when large amount of alkali is contained in SCMs [5], and that volcanic glass contained in *Ito-shirau*; raw material, can prevent alkali-silica reactions [18].

Table 2. Properties of VGP.

Element	VGP5	VGP3	VGP1
Glass content (weight %)	85.7	87.4	88.6
Density (g/cm^3)	2.36	2.38	2.35
BET surface area (m^2/g)	6.49	4.17	15.00
Particle size D50 (μm)	5.1	3.1	1.3
SiO_2 (%)	73.6	73.7	71.4
TiO_2(%)	0.19	0.21	0.22
Al_2O_3	12.30	12.20	12.9
Fe_2O_3	1.49	1.57	2.12
MnO	0.05	0.05	0.06
MgO	0.25	0.28	0.37
CaO	1.35	1.44	1.56
Na_2O	3.73	3.64	3.70
K_2O	4.37	4.38	4.17
P_2O_5	0.03	0.44	0.04
LOI (%)	2.68	2.49	3.42
SiO_2 +Al_2O_3 +Fe_2O_3	87.39	87.47	86.42

Whereas the average particle diameter of VGP 5 is the largest, the BET specific surface of VGP 3 is the smallest, presumably due to being classified by jet mill during recovery by cyclone. As shown in Fig. 5, the particles of VGP 5 have an angular shape and the surface is almost smooth. Hackle marks created by pulverizing process are also observed. On the other hand, lamellar surface is observed on the surface of CF, which might be caused by the weathering of glass.

In regard to setting a density of 2.4 g/cm^3 as a threshold for the glass percentage, X-ray diffraction (XRD) was measured to ascertain the mineral phase and estimate the amount of amorphous materials. XRD was measured using corundum (α-Al_2O_3) with a mean diameter of 3 μm as an internal standard substance at an internal ratio of 20%. In Rietveld analysis, the microabsorption was corrected assuming the diameter of the target minerals to be 5 μm. The target minerals were those contained in the raw material, such as quartz and albite. After selecting the target phase, parameters were refined, and the mineral phase was quantified.

Samples for measurements were prepared by centrifuging VGP 5 and the CF at 10,000 rpm, each into phases under and over a density of 2.4 g/cm^3 using a heavy liquid with a density of 2.4 g/cm^3, filtering the separated phases with membrane filter, and washing repeatedly.

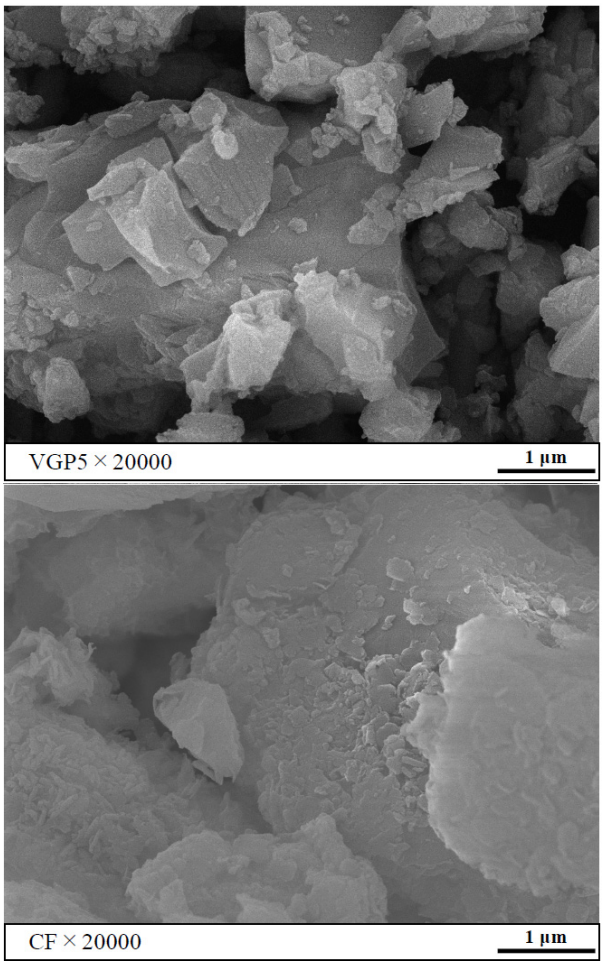

Figure 5. SEM picture of VGP 5 (top) and CF (bottom).

Table 3 and Fig. 6 show the XRD patterns and results of mineral phase quantification, respectively. The amorphous content of VGP 5 with a density of 2.4 g/cm^3 or less is 98.7%, demonstrating that it is high purity volcanic glass. On the other hand, the amorphous content of VGP 5 with a density of more than 2.4 g/cm^3 is 73%, but crystalline minerals such as quartz are also contained. The amorphous content of the CF is also high, but lamellar minerals (clay minerals), such as antigorite, are contained. The density of individual volcanic particles may vary; but it was reported that the ones of pumices are generally between about 0.7 and 1.2 g/m^3, glass shards commonly have densities of 2.35 to 2.45 g/m^3, lithic fragments range from 2.7 to 3.2 g/m^3, and crystals vary from about 2.6 to 5.2 g/m^3 [6]. These results demonstrate that sorting out particles less than 2.4 g/cm^3 by dry gravity concentration and removal of smaller clay fraction by bag filter is technically effective.

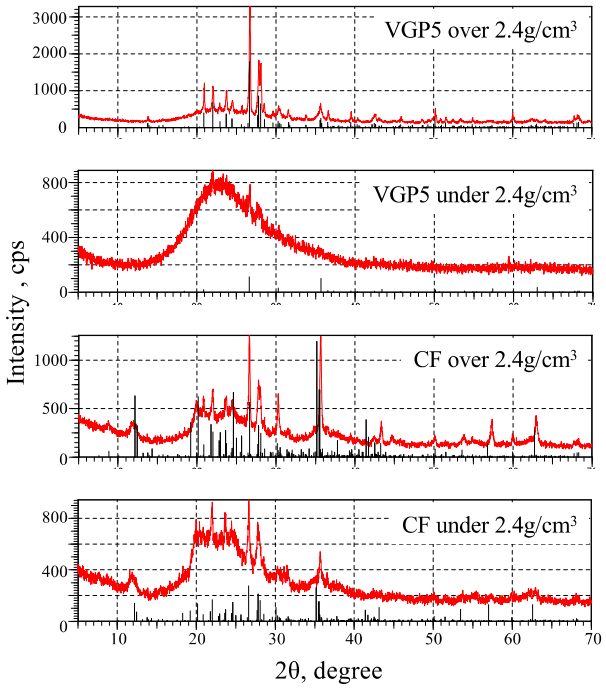

Figure 6. XRD of VGP and CF.

Table 3. Results of Rietveld Analysis.

	VGP5			CF		
	under 2.4	over 2.4	total	under 2.4	over 2.4	total
Content (%)	88.6	11.4	100	62.2	37.8	100
Amorp.	98.7	73.5	95.83	91.9	78.8	86.95
Quartz	-	7.5	0.86	1.2	2.7	1.77
Magnetite	0.1	1.1	0.21	1.1	5.5	2.76
Muscovite	-	-	0.00	-	2.0	0.76
Albite(high)	1.2	17.9	3.10	4.0	8.9	5.85
Antigorite	-	-	0.00	1.8	2.2	1.95

2.3 Mix proportions and test method

The experimental program for three types of VGP was divided into three series, and tests were conducted on concrete mixtures. Table 4 lists the materials used in the experiments. Table 5 shows the factors, levels and mixing proportions. In the first series, to assess the suitability of using VGP to produce high performance concrete, the water-to-binder ratio was kept at 0.2 replacing 10% by mass of low heat Portland cement with VGP. The performance of concrete was evaluated by tests on its fresh and hardened properties compared with that of silica fume concrete. Slump-flow tests were carried out as per JIS A 1150, while the air content was determined by a pressure meter as per JIS A 1128. Compressive strength tests were performed on 100×200-mm water-cured cylinders at 7, 28, 56, and 91 days as per JIS A 1108. Three specimens were used for each test at each age and the average values were reported.

Series II was performed to investigate the effect of VGP on the long-term strength. The water-to-binder ratio was kept at 0.4, while replacing 0% and 30% by mass of normal Portland cement with VGP. Compressive strength tests were performed at 1, 4, 13, 26, and 54 weeks as per JIS A 1108.

In series III, tests on basic durability were conducted on conventional concrete mixtures replacing 0 to 20% by mass of normal Portland cement with VGP 1. The mixture design was controlled within the ranges of water content of around 185 kg/m^3, cement content of less than 300 kg/m^3, and water to binder ratio of around 0.6.

The influence of VGP on the chloride diffusion of concrete is examined by the experiment. Tests were performed according to the JSCE standard "test method for apparent diffusion coefficient of chloride ion in concrete by submergence in salt water". After cutting off 25 mm slices from the top and bottom ends of each cylinder, concrete specimens were cured in a water bath at 20°C. The curing period was 28 days. Specimens were coated with epoxy excepting the circular placing surface and immersed in a 10% NaCl solution at 20°C for 202 days. The total chloride ion profile was determined by cutting four 10 mm slices from each cylinder so that the centers of the slices would be the points at depths of 5, 20, 35, and 50 mm from the uncoated surface. These were crushed to less than 150 μm and subjected to ion chromatography to quantify chloride ions in accordance with JIS A 1154 (Method of test for chloride ion content in hardened concrete).

Table 4. Materials used.

Material		Properties	Marks	
Binder	Cement	Normal Portland cement Density: 3.24 g/cm^3	N, NPC	
		Low-heat Portland cement Density: 3.24 g/cm^3	L, LPC	
	VGP	VGP5, VGP3, VGP1	VGP	SCM
	Silica fume	Specific surface area: 16.0m^2/g SiO_2: 93.76%, MgO: 0.58%, SO_3: 0.27% LOI: 1.91%, density: 2.25 g/cm^3	SF	
Fine aggregate		Crushed lime, density: 2.67g/cm^3	S1	
		Crushed tight sand, density: 2.62 g/cm^3	S2	
Coarse aggregate		Crushed tight sand, density: 2.64 g/cm^3	G1	
		Crushed lime, density: 2.70 g/cm^3	G2	
Chemical admixture		high-range water-reducing admixture	SP1	
		air-entraining and high-range water-reducing admixture	SP2	
		air-entraining and water reducing admixture	SP3	
		air-entraining admixture	AE	

Carbonation studies were carried out using column specimens according to JIS A 1153 (Method of accelerated carbonation test for concrete). As preliminary curing, specimens were water-cured at 20°C after demolding until an age of 4 weeks and then left to stand in a thermo-hygrostatic chamber at 20°C and 60% R.H. until an age of 8 weeks. These were then kept in an accelerated carbonation testing equipment at 20°C and 60% R.H. with a CO_2 concentration of 5% until accelerated test ages of 1, 4, 8, 13, and 26 weeks for carbonation depth measurement using phenolphthalein.

Table 5. Factors and level, mixing proportions.

Series	W/B	Cement	W (kg/m^3)	SCM/B (%)	S1:S2	s/a (%)	SCM used	Chemical admixture used	Target air content (%)	Target slump (cm)
Ⅰ	0.20	L	160	10	4:6	45.2	SF VGP1 VGP3 VGP5	SP1	2.0±1.0	Flow value 65±10
Ⅱ	0.40	N	180	30	2.5:7.5	42.8	VGP1 VGP3 VGP5	SP2+AE	5.0±1.0	Slump value 18±2.5
Ⅲ	0.61	N	183	0 10 20	2.5:7.5	50.8	VGP1	SP3+AE	5.0±1.5	Slump value 18±2.5

3 Results of concrete tests and discussion

3.1 Series I: high performance concrete

Table 6 gives the fresh properties immediately after mixing and chemical admixture dosage. Fig. 7 shows changes in the slump flow and air content over time. Fig. 8 shows the time to the end of flow and time to 50 cm diameter. VGP 1 is found to provide a slump flow comparable to SF with a smaller chemical admixture dosage. The time to the end of flow and time to 50 cm diameter implied similar viscosity, with changes in fresh performance being also similar. On the other hand, VGP 3 and VGP 5 provided greater slump flow than SF with a lower superplasticizer dosage, but the viscosity of the resulting fresh concretes was too high for practical use as suggested by the time of flow stop and 50 cm flow.

Table 6. Results of fresh concrete.

Mark	Flow value (cm)	Air content (%)	Time to flow to a diameter of 50cm (sec)	Time to end-of-flow (sec)	SP1 content in percentage by weight of B
SF	69.5	2.5	6.8	88	1.6%
VGP1	70.8	2.9	7.8	64	1.4%
VGP3	81.2	2.4	9.8	118	1.3%
VGP5	77.7	2.3	21.0	161	1.3%

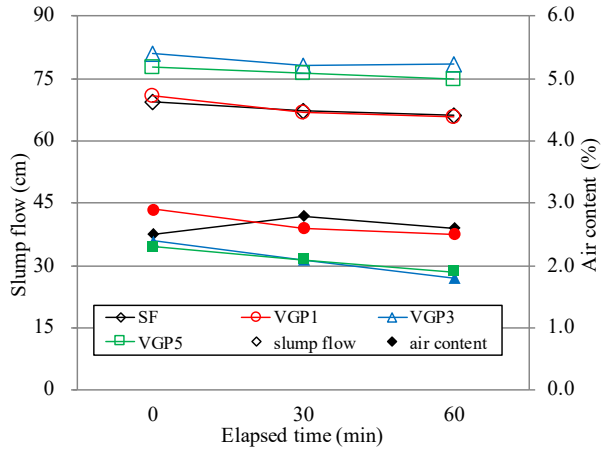

Figure 7. Slump flow and air content.

Fig. 9 shows the particle size distribution of the binders used measured by laser equipment. Fig. 10 shows the packing ratio of binders calculated from the particle size distribution using a particle packing simulation program [14]. When compared with the binder solely consisting of low-heat Portland cement, the packing ratio of VGP 1 was high up to a replacement ratio of 10%, whereas those of VGP 3 and VGP 5 was almost the same level with control. Water retained between binder particles decreases as the packing ratio of the binder increases, improving the workability of the mixture such as UHPC by the micro filler effect.

These calculation results suggest that VGP 1 in place of 10% to 30% of LPC may produce such an effect when water to binder ratio is less than 0.2, but VGP 3 and VGP 5 will not achieve the effect even by adjusting the replacement ratio.

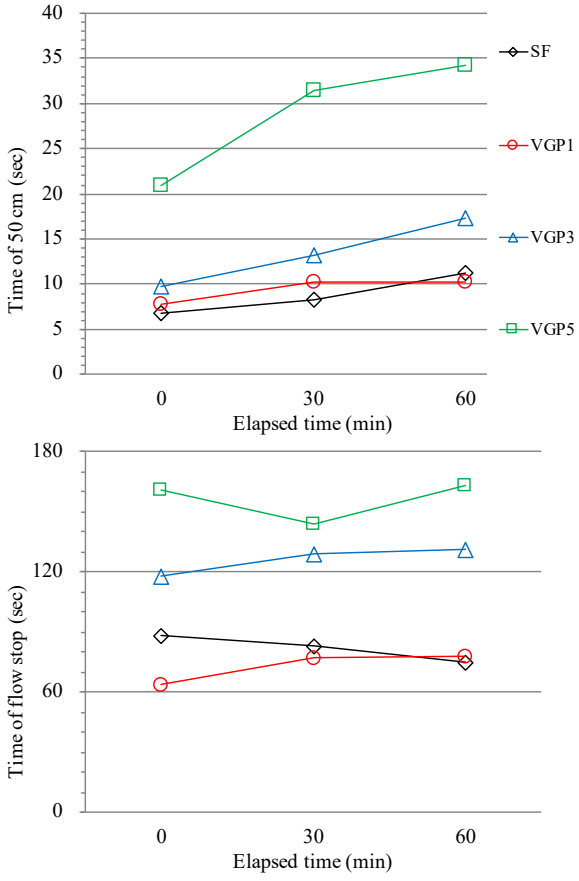

Figure 8. Time of 50cm flow (top) and flow stop (bottom).

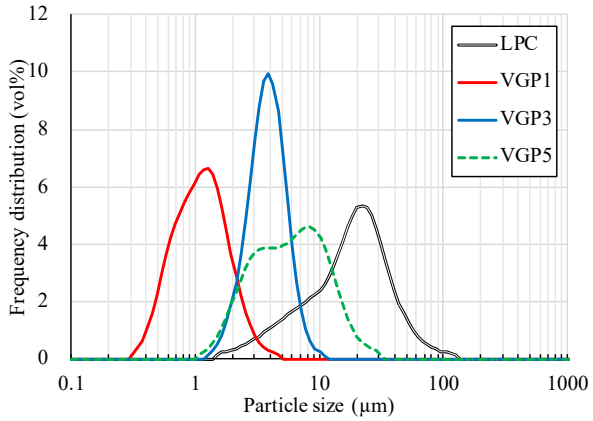

Figure 9. Particle size distribution of binders.

Fig. 11 shows the results of interparticle distance (edge to edge) distribution of a mixture with a W/B of 0.2, in which 10% of LPC was replaced with VGP, using the same simulation program. Table 7 shows the results of average interparticle distance and average coordination number of particles. While the mean interparticle distance of VGP 1 was calculated to be 0.33 μm, those of VGP 3 and VGP 5 were 0.24 μm, being 72% of VGP 1. And the coordination number of VGP1 mixture was the least. The combination of binders with a longer time to the end of flow turned out to be the combination with a smaller interparticle distance and larger coordination number.

A short interparticle distance and a large number of particles therefore leaves a limited space for the rotational motion of binder particles to make the paste flow. It is therefore inferred that the interparticle distance and coordination number is a key factor for the fluidity improving effect (micro filler effect) in addition to the packing ratio.

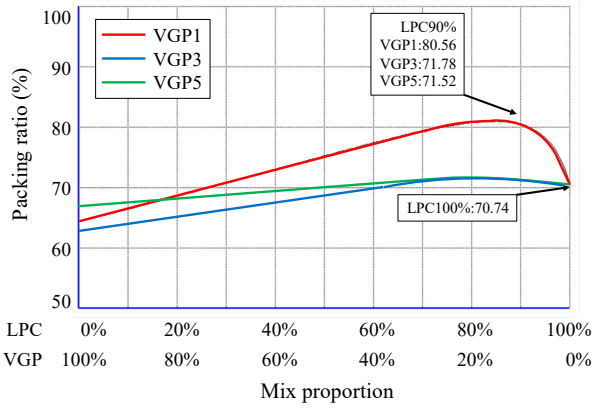

Figure 10. Calculated packing ratio.

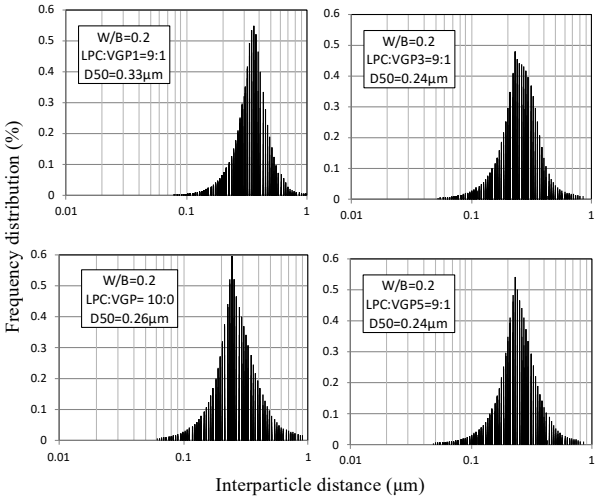

Figure 11. Calculated interparticle distance.

Table 7. Results of calculation.

	Packing ratio (%)	Average interparticle distance, edge to edge (μm)	Average coordination number of particles
VGP1	80.56	0.33	7.40
VGP3	71.78	0.24	8.12
VGP5	71.52	0.24	7.88

In comparison with SF with a mean diameter of 0.1 μm, the size of VGP is large. However, it can be said that VGP is a supplementary cementitious material that is expected to produce a sufficient effect of improving the workability of low W/B mixtures as demonstrated in the present results, provided that its physical properties including grading are rectified during the process of crushing and classification and that impurities including clay minerals are removed.

Fig. 12 shows the results of compression tests to an age of 13 weeks. The compressive strength of VGP 1 with a BET of 15m^2/g, which was similar to SF, exceeded SF at 1 week and was equivalent to SF at 4 weeks and thereafter. The SiO_2 content of VGP 1 is 70%, being lower than SF's 95%, the content of $SiO_2 + Al_2O_3 + Fe_2O_3$, which are active ingredients of natural pozzolans specified in ASTM C 618, is as high as 86%. This composition and the BET specific surface comparable to SF, as well as the filler effect due to the enhanced packing ratio, presumably led to the strength development of VGP 1 beginning form 1 week.

Fig. 13 shows the result of mercury intrusion porosimetry to ascertain the pore structure and porosity. Specimens were mortar mixture replacing 0% and 10% by mass of normal Portland cement with VGP1 with 0.3 water to binder ratio, and tests were performed at water curing ages of 7days and 28 days. VGP1 mortar showed slightly lower porosity compared with NPC mortar from 7 days. And, cumulated partial pore volume ratio of 3 nm-10 nm ranged diameter started increasing from 7 days, whereas that of 10 nm-300 μm raged diameter started decreasing. This is presumably caused by both the filler effect and pozzolanic reaction, and this denser structure may lead to greater compressive strength.

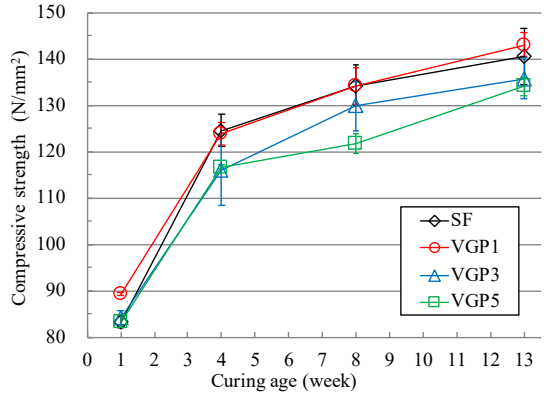

Figure 12. Compressive strength (W/B=0.2).

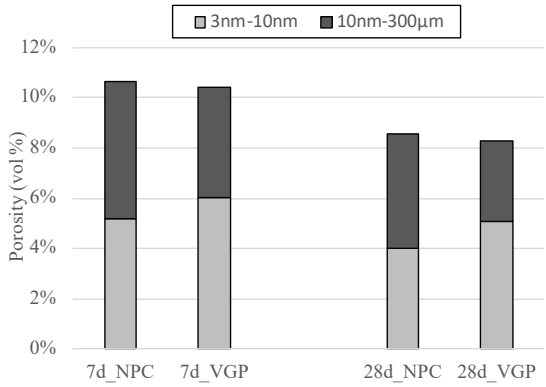

Figure 13. Porosity calculated from MIP date.

The strength test results of VGP 3 and VGP 5 were lower than those of SF at all ages. The chemical compositions of the three types of VGPs are nearly the same, and the only difference of their physical properties is the fineness. VGP 3 and 5 with low BETs are presumably prone to slow reaction, while their low packing ratios may adversely affect the strength development.

3.2 Series II: Long-term strength of concrete

Fig. 14 shows the compression test results to 54 weeks. The compressive strength of VGP 1 exceeded that of control concrete from an age of 1 week, kept active development until 4 weeks, and retained moderate gains until 26 weeks. The strength scarcely increased from 26 to 54 weeks, suggesting that the ultimate strength is reached. The strength of VGP 3 was lower than that of control concrete up to 4 weeks but surpassed the control at 13 weeks, and retained marginal gains until 54 weeks. Its reaction was therefore considered to proceed over a long time. The strength of VGP 5 developed to a level comparable to the control at 13 weeks and kept slight increase thereafter similarly to NPC. Recent study showed that compared with 17 µm, using a smaller sized 6 µm volcanic ash result in a denser pore structure, and thus a greater compressive strength at curing age of 4 weeks [16].

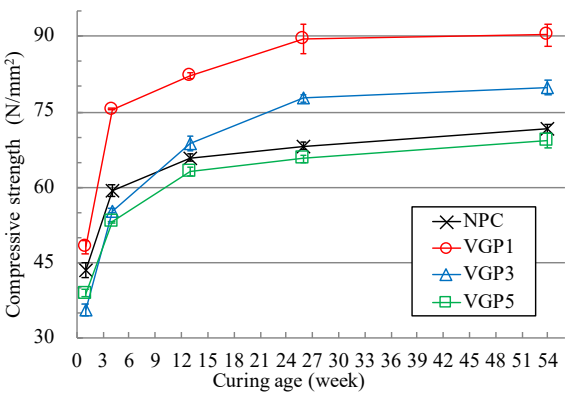

Figure 14. Compressive strength (W/B=0.4).

These results along with the results of series I demonstrate that, within the range of the present tests, on one hand the reaction of mixtures with a BET specific surface of around 10m^2/g or less proceeds more slowly than that of SF but their pozzolanic reaction keeps proceeding over a long time after 4 weeks. On the other hand, when crushed to a mean diameter of 1 µm and BET of 15 m^2/g, it turns into a supplementary cementitious material that contributes to strength beginning from 1 week.

3.3 Series III: Basic durability properties (VGP 1)

Fig. 15 shows the results of compression tests until 13 weeks. The strength increased as the VGP 1 replacement ratio increased. Fig. 16 and 17 show SEM image and EDX mapping of NPC specimens and VGP1 specimens just after compression test at 13 weeks, respectively. Table 8 shows results of Ca/Si ratio calculated by SEM-EDX analysis.

It was reviewed that the C-S-H phase in blended cements usually displays Ca/Si ratios in the range of lower than 1 to 1.8, i.e., lower than the observed C-S-H Ca/Si range in normal Portland cement [5]. In the present tests, it is presumed that reduced Ca/Si ratio result in finer pore size distribution, lower permeabilities and chemically more resistant on conventional concrete mixtures.

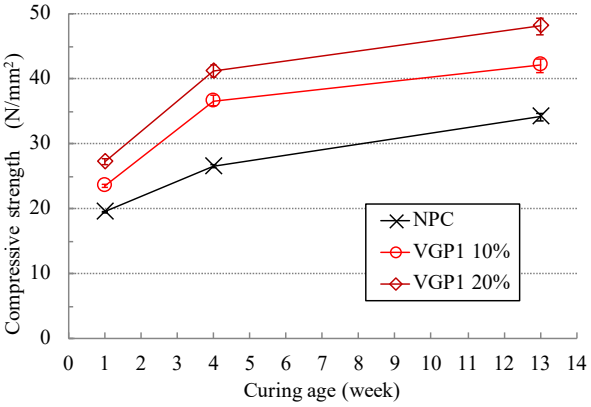

Figure 15. Compressive strength (W/B=0.6).

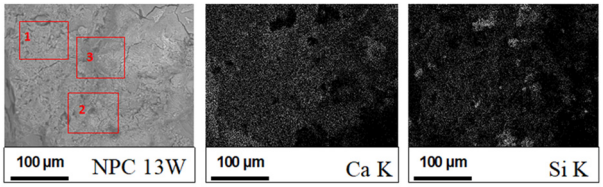

Figure 16. SEM picture of NPC specimens and EDX maps for Ca and Si at ×500 magnification.

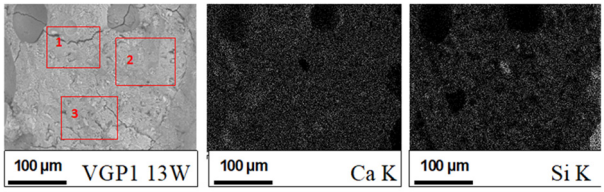

Figure 17. SEM picture of VGP1 specimens and EDX maps for Ca and Si at ×500 magnification.

Table 8. Results of fresh concrete.

	Sampling number	Average of Ca/Si	Standard deviation
NPC 13W	13	3.24	1.38
VGP1 13W	17	1.56	0.55

Fig. 18 shows the total chloride ion concentration profile in concrete. When the replacement ratio is 10%, the surface concentration is slightly higher than that with 0%. This is presumably because chloride ions scarcely permeate deeper and accumulated near the surface. With a replacement ratio of 20%, however, chloride ion penetration is inhibited even in the surface region. Here, the total chloride ions on the concrete surface and the apparent diffusion coefficient of chloride ions by immersion tests were simultaneously calculated by regression analysis of the values of the total chloride ions measured at each depth of each specimen using the solutions of diffusion equation based on Fick's second law. The apparent diffusion coefficients to three significant digits by rounding off the fourth digit shown in the figure are as low as 15% and 10% with replacement ratios of 10% and 20%, respectively, demonstrating VGP 1's excellent chloride penetration resistance.

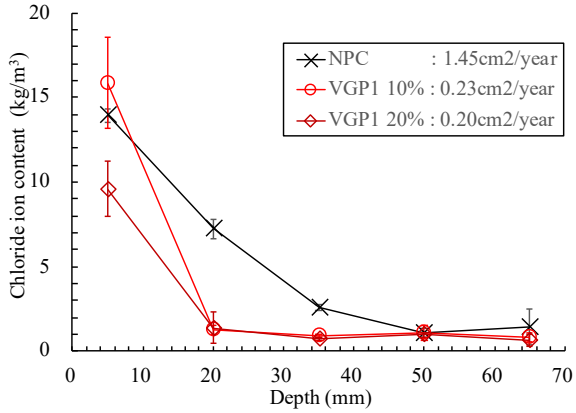

Figure 18. Total chloride concentration profile.

According to a study [15] dealing with 2-year immersion tests on concrete containing silica fume with a W/B of 0.35 to 0.50 and replacement ratios of 0, 4, and 8% conforming to the same JSCE specifications, the apparent diffusion coefficient decreases to 40% and 20% with replacement ratios of 4% and 8%, respectively, with small scatters depending on the W/B. Analysis by MIP reveals correlation between reductions in the pore volume 10 nm or more in diameter and diffusion coefficients, which are presumed to be due to pozzolanic reaction and the micro filler effect.

JSCE specifies that the period of water curing prior to immersion be 4 weeks. Therefore, the reaction of VGP 1 is considered to have sufficiently proceeded by the end of 4 week curing similarly to SF. The results of strength tests including series I and II are consistent with these results.

Fig. 19 and 20 show the results of accelerated carbonation tests. The square root of the age during acceleration is found to be linearly related to the carbonation depth. The equations of the approximated straight lines shown in the figure demonstrate that the carbonation rate coefficient of specimens with 10% replacement is slightly lower, and that of specimens with 20% replacement is 8% higher, than the control specimens, both being nearly of the same level. It is pointed out that pozzolanic materials in place of part of cement generally reduces the carbonation resistance of concrete due to the lower quantity of Portland cement and calcium hydroxide consumption by pozzolanic reaction [17], however the reduced permeability might render blended cements counteracts the loss of buffering $Ca(OH)_2$ [1]. In the present tests, it is presumed that the effect of pore structure densification offsets the effect of CH consumption by pozzolanic reaction, when reaction begins at an early age.

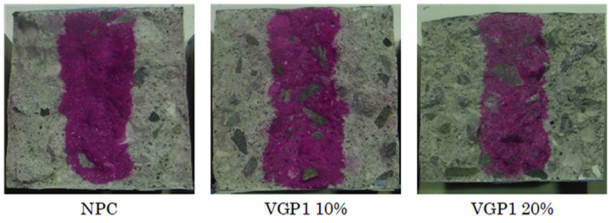

Figure 19. Results of phenolphthalein tests at accelerated age of 26 weeks.

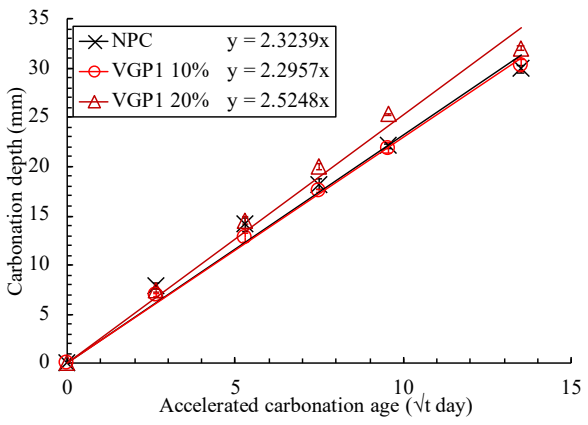

Figure 20. Carbonation depth and accelerated age.

4 Conclusions

The following were found in this study:

(1) When utilizing volcanic ejecta for engineering purposes in the concrete field, the fraction with a density 2.4 g/m^3 or less is found effective from the aspect of the inclusion of clay minerals. High-purity volcanic glass can be separated from natural pyroclastic flow deposits using equipment referred to as a gravity separator.

(2) Separated volcanic grass contains 70% of SiO_2, and the fraction with a density of 2.4 g/m^3 or less is 85% or more. When crushed to a mean diameter of 1 µm and BET of 15 m^2/g, it turns into a supplementary cementitious material that contributes to strength beginning from 1 week in the W/B range of 0.2 to 0.6.

(3) With a low W/B of around 0.2, concrete containing volcanic glass powder with optimized physical properties demonstrates strength and mobility performance equal to or higher than concrete containing SF. With a high W/B of around 0.6, it improved basic durability performance of concrete.

In Japan, all silica fume is imported from abroad. Assuming recoverable reserves of *Ito-shirasu* (estimated to have a volume of 75 billion m^3) to be 20%, as recovery rate of volcanic glass from raw material is around 45%, we can manufacture 7.4 billion tons of VGP (bulk density 1.1 ton/m^3). In 2017, about 83 million m^3 of concrete is manufactured in Japan. Regarding average cement content as 300 kg/m^3, 7.4 billion tons of VGP can be replaced 30% by mass of Portland cement for 100 years. Additionally, volcanic ejecta like *Ito-shirasu* is found in various regions in Japan. If these volcanic ejecta turns from unutilized natural resource to high-performance SCMs, it will contribute to reduction of CO_2 emissions and durability of concrete in the future.

Acknowledgements

The authors express their thanks to Dr. Y. Aikawa at Tokyo Institute of Technology for his assistance regarding the calculation of packing ratios and interparticle distances.

References

[1] K. Kupwade-Patil, C. de Wolf, S. Chin, J. Ochsendorf, AE. Hajiah, A. Al-Mumin, O. Büyüköztürk, Impact of Embodied Energy on materials/buildings with partial replacement of ordinary Portland Cement (OPC) by natural Pozzolanic Volcanic Ash, J Clean Prod (2018) 177: 547-554. https://doi.org/10.1016/j.jclepro.2017.12.234

[2] I. Hiroi, The Preparation and Use of concrete Blocks for Harbour Works, Transactions, ASCE (1904) LIV. Part A (10): 211-220.

[3] I. Hiroi, On Long-time Tests of Portland Cement, Hydraulic Lime, and Volcanic Ashes, J College Engrg, Tokyo Imperial Univ (1920) X (7): 155-172.

[4] G. Cai, T. Noguchi, H. Degée, J. Zhao, R. Kitagaki, Volcano-related materials in concretes: a comprehensive review, Environ Sci Pollut Res (2016) 23 (8): 7720-7243. https://doi.org/10.1007/s11356-016-6161-z

[5] R. Snellings, G. Mertens, J. Elsen, Supplementary Cementitious Materials. Rev Mineral Geochem (2012) 74 (1): 211-278. https://doi.org/10.2138/rmg.2012.74.6

[6] S. Shipley, A. M. Sama-Wojcicki, Maps Showing Distribution, Thickness, and Mass of Late Pleistocene and Holocene Tephra from Major Volcanoes in the Pacific Northwest of the United States; a Preliminary Assessment of Hazards from Volcanic Ejecta to Nuclear Reactors in the Pacific Northwest (1983), USGS, MF-1435.

[7] R. Snellings, Assessing, Understanding and Unlocking Supplementary Cementitious Materials, RILEM Tech Lett (2016) 1 (1): 50-55. https://doi.org/10.21809/rilemtechlett.2016.12

[8] K. Takewaka, Characteristics of SHIRASU Concrete, Concr J , JCI (2007) 45 (2): 16-23.

[9] Winners of the 2017 ACI Excellence in Concrete Construction Awards, Concr International (2017) 39 (11): 18-24.

[10] A. Tomoyose, T. Noguchi, K. Sodeyama, K. Higashi, Experimental study on using differentiated shirasu by gravity concentration and classification as concrete material, CAJ Proc Cem Concr (2016) 70 (1): 580-587.

[11] A. Tomoyose, T. Noguchi, K. Sodeyama, K. Higashi, Stability of volcanic silicate powder for concrete manufactured from shirasu through gravity classification and pulverization, CAJ Proc Cem and Concr (2017) 71 (1): 674-681.

[12] K. Sodeyama, A. Tomoyose, T. Noguchi and K. Higashi, Total Utilization of Shirasu as Construction Materials through Dry Gravity Classification and Pulverization, J Soc Mat Sci, Japan (2017) 66 (8): 574-581. https://doi.org/10.2472/jsms.66.574

[13] A. Tomoyose, T. Noguchi, K. Sodeyama and K. Higashi, Fundamental study about volcanic glass classified from Ito-shirasu by gravity classification, Proc Jpn Concr Ins (2017) 38 (1): 151-156.

[14] Y. Aikawa, M. Inoue, E. Sakai, Fundamental Theory of Void Fraction of Cohesive Spheres with Size Distribution and Its Application to Multi Component Mixture System, J Cer Soc Jpn (2012) 120 (1397): 21-24. https://doi.org/10.2109/jcersj2.120.21

[15] S. Kawahara, T. Saeki, T. Shima and H. Yoshizawa, Fundamental Study on Chloride Ion Diffusion and Steel Corrosion in Silica Fume Concrete, CAJ Proc Cem and Concr (2011) 65 (1): 360-367.

[16] K. Kupwade-Patil, S. H. Chin, M. L. Johnston, J. Maragh, A. Masic, O. Buyukozturk, Particle size effect of volcanic ash towards developing engineered portland cements, J Mater Civil Engrg ASCE (2018) 30 (8): 04018190. https://doi.org/10.1061/(ASCE)MT.1943-5533.0002348

[17] K. Sisomphon, L. Franke, Carbonation rates of concrete containing high volume of pozzolanic materials, Cem Concr Res (2007) 37 (12): 1647-1653. https://doi.org/10.1016/j.cemconres.2007.08.014

[18] K. Takewaka, State-of-the-Art-Report on Characteristics of SHIRASU Concrete and its Practical Use, Concr J, JCI (2014) 42 (3): 38-47

[19] H. Choi, T. Noguchi, A. Tomoyose and T. Ito, Experimental study on application of Ito-shirasu concrete to buildings, Proc Jpn Concr Ins (2015) 37 (1): 73-78.